Polyester derived from recycled poly(ethylene terephthalate) waste for regenerative medicine†

Kishor Sarkar,[a] Sai Rama Krishna Meka,[b] Amrit Bagchi,[b] N. S. Krishna,[c] S. G. Ramachandra,[c] Giridhar Madras[a] and Kaushik Chatterjee*[b]

Despite advances in regenerative medicine, the cost of such therapies is beyond the reach of many patients globally in part due to the use of expensive biomedical polymers. Large volumes of poly(ethylene terephthalate) (PET) in municipal waste is a potential source of low cost polymers. A novel polyester was prepared by a catalyst-free, melt polycondensation reaction of bis(hydroxyethylene) terephthalate derived from PET post-consumer waste with other multi-functional monomers from renewable sources such as citric acid, sebacic acid and D-mannitol. The mechanical properties and degradation rate of the polyester can be tuned by varying the composition and the post-polymerization time. The polyester was found to be elastomeric, showed excellent cytocompatibility *in vitro* and elicited minimal immune response *in vivo*. Three-dimensional porous scaffolds facilitated osteogenic differentiation and mineralization. This class of polyester derived from low cost, recycled waste and renewable sources is a promising candidate for use in regenerative medicine.

1. Introduction

It is widely believed that engineered tissues could revolutionize medicine and offer promising new treatments for many debilitating diseases. In tissue engineering, a scaffold should ideally be non-toxic, biodegradable, and highly porous with interconnected architecture to support cell attachment, proliferation and extra-cellular matrix (ECM) production to ultimately facilitate tissue generation. In addition, it should possess optimal mechanical and physical properties.[1-4] The currently available library of such materials is limited and expensive adding to the already high costs of these emerging therapies. There is a need for biomedical polymers derived from low cost, renewable sources and recycled waste that could offer cost effective solutions.

The use of PET has greatly increased because of its widespread application in packaging of food and drinks. This has resulted in an ever-growing volume of post-consumer and industrial PET waste. Therefore, recycling of waste PET has become a significant global challenge.[5,6] PET can be recycled by various techniques such as glycolysis, aminolysis and hydrolysis.[7-9] For recycling of PET, glycolysis is economically advantageous over the other chemolysis processes.[10] The objective of this work was to prepare polymers for regenerative medicine using recycled PET as a source. PET fabrics have been used clinically for over five decades in vascular grafts. However, non-biodegradable PET is not well suited for preparation of scaffolds for tissue regeneration. The hydroxyl-terminated monomer, bis(hydroxyethylene) terephthalate (BHET) prepared by glycolysis of PET has been used as a raw material for preparing various polymers such as polyurethanes, unsaturated polyesters, epoxy resins, and UV curable films[11-14] and was utilized in this study.

In this study, we report the synthesis and characterization of a novel class of biodegradable BHET-based polyester for biomedical applications. BHET is soluble in hot water. It has not been used in biomedical applications and its toxicity is not reported. The polyester elastomer was synthesized using BHET with multi-functional monomers from renewable sources such as citric acid (CA), sebacic acid (SA) and D-mannitol (MA). The terminal active primary hydroxyl groups of BHET can react with carboxylic acid groups to form ester linkage. The aromatic ring located at the centre of BHET contributes to the rigidity and strength of the polymer. SA and CA were used as the source of carboxylic acid groups. SA and CA are known to be non-toxic and have been successfully used as biomedical polymers.[15-18] Acetyl-CoA and succinyl CoA are degraded products of SA in the Krebs cycle and CA is also an intermediate in the Krebs' cycle.[19,20] Apart from this, MA is an intermediate product of carbohydrate metabolism and it is metabolized in an insulin-independent manner.[21] This BHET–CA–SA–MA (BCSM)

[a] Department of Chemical Engineering, Indian Institute of Science, C. V. Raman Avenue, Bangalore 560012, India

[b] Department of Materials Engineering, Indian Institute of Science, C. V. Raman Avenue, Bangalore 560012, India. E-mail: kchatterjee@materials.iisc.ernet.in; Tel: +91-80-2293-3408

[c] Central Animal Facility, Indian Institute of Science, C. V. Raman Avenue, Bangalore 560012, India

† Electronic supplementary information (ESI) available. See DOI: 10.1039/c4ra09560j

polyester offers many potential advantages. BHET is obtained by recycling PET waste, and is thus, eco-friendly. All the other monomers are also easily available from renewable sources and are non-toxic. The synthesis process is solvent and catalyst free, simple and economical. Moreover, the mechanical properties, water wettability and degradation rate can be tuned by varying the monomer fractions and the duration of post-polymerization.

2. Experimental section

2.1. Materials

Commercial consumable PET bottles (Pearl Polymers Limited, New Delhi, India) were used. The bottles were cut into approximately 5×5 mm^2 flakes and subsequently cleaned with weak detergent solution followed by washing and drying. Zinc acetate, ethylene glycol and mannitol were purchased from S. D. Fine Chemicals. Sebacic acid, (3-(4,5-dimethylthiazol-2-yl)-2,5-diphenyltetrazolium bromide) (MTT) and Alizarin Red S were obtained from Sigma-Aldrich. Sodium chloride and citric acid were purchased from Merck. Alpha-modification of Minimum Essential Medium (α-MEM), foetal bovine serum (FBS), penicillin–streptomycin, L-glutamine and trypsin–EDTA were obtained from Invitrogen. All other chemicals were analytical grade and used as received.

2.2. Preparation of BHET from PET waste

BHET was prepared by depolymerisation of PET as reported previously with minor modifications.[22] Briefly, 30 g of PET flakes, 100 g of ethylene glycol (EG) and 0.3 g of zinc acetate (as a *trans*-esterification catalyst) were charged in a three-necked 500 mL round-bottom flask equipped with a thermometer, a reflux condenser and a magnetic stirrer. The depolymerization reaction was performed at 198 °C for 8 h under nitrogen atmosphere. The reaction mixture was then cooled to room temperature and 500 mL of distilled water was added under vigorous stirring. After filtration, the solid cake was dispersed in hot water and boiled for 1 h with constant stirring to extract the BHET as it is soluble in hot water.[23] The boiling solution was filtered rapidly to separate the oligomer fraction from the BHET. The filtrate was cooled to room temperature and then placed at 4 °C for 24 h. BHET in the form of needle-shaped crystals was obtained after filtration and dried at 40 °C for 24 h.

2.3. Synthesis of polyester

To synthesize the polyester, BHET, SA, CA and MA were used as the monomers. The polyester was synthesized by melt-condensation polymerization process as reported previously.[24] The composition of monomers for different polyester synthesis is shown in Table 1. BHET, SA and CA were taken in a three-neck 100 mL round-bottom flask. After purging with nitrogen gas, the flask was heated to 160 °C with constant stirring. The reaction was continued at this temperature under nitrogen flow to remove the water obtained as by-product during reaction for 90 min. MA was added to the mixture and the reaction was allowed to continue for 30 min. The pre-polymer was removed from the

Table 1 Chemical composition, physical properties and mechanical properties of the different polyester elastomers

| Sample | Composition (molar ratio) | | | | Curing time (days) | Young's modulus (MPa) | Tensile strength (MPa) | Elongation at break (%) | Scaffold density (g cm^{-3}) | Scaffold porosity (%) | Contact angle (degrees) |
	BHET	CA	SA	MA							
BCSM-1	0.5	0.5	1.0	0.25	5d	3.03 ± 0.05	3.27 ± 0.18	139 ± 6	0.126 ± 0.01	85 ± 5	60.5 ± 3.3
BCSM-2	1.0	0.5	1.0	0.25	3d	0.16 ± 0.04	0.42 ± 0.08	389 ± 28	—	—	68.7 ± 2.8
					4d	1.05 ± 0.04	1.27 ± 0.02	158 ± 24	—	—	72.8 ± 3.5
BCSM-3	2.0	0.5	1.0	0.25	5d	1.84 ± 0.05	2.31 ± 0.23	168 ± 11	0.102 ± 0.01	86 ± 5	76.9 ± 2.9
					5d	0.15 ± 0.035	0.49 ± 0.068	607 ± 4	0.108 ± 0.01	84 ± 6	85.4 ± 5.1

flask after cooling. Finally, the pre-polymer was taken in a Teflon Petri dish and cured at 120 °C for different time intervals (2, 3, 4 and 5 days) for post-polymerization.

The pre-polymer was purified before characterization by NMR and gel permeation chromatography (GPC). The pre-polymer was washed with distilled water to remove unreacted water soluble monomers CA and MA followed by washing with hot water to remove unreacted BHET. Subsequently, the pre-polymer was dissolved in acetone and re-precipitated in water/ iso-propanol mixture to remove unreacted SA as SA is soluble in iso-propanol whereas the pre-polymer is insoluble in water. The purified pre-polymer was obtained by repeating the solution precipitation method thrice.

2.4. Characterization of polyester

All post-polymerized polyesters were characterized by attenuated total reflection (ATR) Fourier transform infrared (FT-IR) spectrophotometer (Perkin Elmer Spectrum 100 FT-IR spectrometer). The infrared spectra were recorded at the frequency range of 4000–500 cm^{-1} with 42 consecutive scans at a 4 cm^{-1} resolution. ^{1}H and ^{13}C nuclear magnetic resonance (^{1}H and ^{13}C NMR, Bruker NMR) spectra of the pre-polymers were recorded at 400 MHz using acetone d6 as solvent and tetramethylsilane (TMS) as internal reference. The molecular weight of pre-polymer was determined by gel permeation chromatography (Waters). X-ray diffraction spectrometry of the polyesters in the film form was performed by a wide angle X-ray scattering diffractometer (Panalytical X-ray diffractometer) with Cu Kα radiation ($\lambda = 1.544$) in the range 5–60° (2θ) at 40 kV and 30 mA. Differential scanning calorimetry (DSC, Mettler Toledo DSC1) thermograms were recorded in the range of −40 °C to +250 °C at a heating rate of 10 °C min^{-1}. The mechanical properties of the post-polymerized polyesters were evaluated using a Universal Testing Machine (Mecmesin) equipped with data acquisition software at room temperature according to ASTM D 638 standards. Six specimens were tested for each polymer. The contact angles of the polyester were measured by sessile drop method on a goniometer using ultrapure water as the liquid phase. For contact angle measurements, a small drop of water was placed by a micro syringe on the polymer film and simultaneously the contact angle at the liquid–solid interface was determined by measuring the angle made with the tangent using a calibrated angular scale. At least six measurements were carried out with each polymer at random locations.

2.5. *In vitro* degradation

The *in vitro* degradation of the polymers (10 × 10 × 1 mm^3 sample dimensions) was studied in phosphate buffered saline solution (PBS, 100 mL, pH 7.4). After regular intervals, the polymer sample was taken out from PBS and dried in a hot air oven at 60 °C until a constant weight was achieved. PBS was replaced at every time period to avoid auto-acceleration of hydrolysis. All measurements were performed in triplicate. The percent degradation was calculated by using the following equation:

$$\% \text{ mass remaining} = \frac{M_t}{M_0} \times 100$$

where, M_t and M_0 are the mass of polymer at time t and before the experiment, respectively.

2.6. Fabrication of 3D porous scaffold

The porous 3D scaffolds were fabricated using solvent casting followed by particulate leaching method according to our previous study.[25] The pre-polymer was dissolved in dioxane at concentration of 0.2 g mL^{-1}. Scaffolds (3 mm height × 6 mm diameter) were fabricated in 96 well plates by mixing 100 μL of the pre-polymer solution with 0.13 g of NaCl crystals sieved to 250–425 μm size range. Plates were air-dried for 1 day to remove solvent and placed in an oven at 120 °C for post-polymerization. Then the salt particulate was leached in water for 4 days with daily water changes, freeze-dried (Labconco) and stored under vacuum until use.

2.7. Characterization of scaffolds

The microstructure of the porous scaffolds was observed with an emission scanning electron microscope (FEI ESEM Quanta 200) after sputter-coating with gold for 6 min. The density and porosity of the scaffolds were measured by liquid displacement method.[26] Ethanol was used as the displacement liquid. Salt leached scaffold of weight W was taken in a small graduated measuring cylinder containing known volume (V_1) of ethanol. After keeping the scaffold for 10 min in ethanol, ethanol penetration was carried out by centrifugation. Then the volume of ethanol having immersed scaffold was recorded as V_2. The volume of ethanol after removing of ethanol-impregnated scaffold was recorded as V_3. The volume differences ($V_2 - V_1$) and ($V_1 - V_3$) were the volume of the scaffold skeleton and the volume of entrapped ethanol in the scaffold, respectively. Therefore, the total volume of the scaffold was ($V_2 - V_3$). The density (δ) and porosity (ε) of the scaffold were calculated according to the following equations:

$$\delta = \frac{W}{V_2 - V_3}$$

$$\varepsilon = \frac{V_1 - V_3}{V_2 - V_3}$$

Three measurements of each material were taken for an average value to calculate the density and porosity of the scaffolds.

2.8. Cell proliferation and viability assay

2.8.1. Cell culture. MC3T3-E1 subclone 4 mouse cells (ATCC, USA), a well-characterized osteoblast model,[27] were used for cell culture. The cells were cultured in α-MEM supplemented with 10% (v/v) FBS, 1% penicillin–streptomycin and 1% of 2 mM L-glutamine. The cells were maintained in 5% CO$_2$ at 37 °C

(Thermo Scientific). The cells were harvested at 70–80% confluency using 0.05% trypsin–EDTA for further sub-culturing.

2.8.2. Cell seeding on polymer films and scaffolds. BCSM-2_5d polyester films were cut into small pieces (5 × 5 mm^2 and 1 mm thickness) and placed in 6 well plates. 3D scaffolds were prepared in 48 well plates. All plates were sterilized with ethylene oxide (Anaprolene) and degassed under vacuum for 3 days. Prior to cell seeding, the films and scaffolds were incubated in culture medium for 1 day. 6.0×10^4 cells per well and 1.5×10^4 cells per well were seeded on the polymer films and the scaffolds, respectively. To observe the cell attachment and cell morphology, cells were fixed with 3.7% formaldehyde, washed with PBS and subsequently dried with 30%, 50%, 70%, 90% and 100% ethanol gradients prior to imaging by SEM.

2.8.3. MTT assay. Cell attachment and proliferation on the scaffolds was quantified by methylthiazoletetrazolium (MTT) assay at 1 and 7 days, respectively. The medium was removed and 20 μL of MTT solution (5 mg mL^{-1}) in DMEM media was added to each well. After further incubation for 4 h at 37 °C, the media was removed and replaced with 100 μL DMSO to dissolve the MTT formazan crystals. The absorbance was recorded at 570 nm by a microplate reader (BioTek). The cell viability (%) was calculated according to the following equation:

$$\text{Cell viability } (\%) = \frac{\text{OD}_{570(\text{Sample})}}{\text{OD}_{570(\text{Control})}} \times 100$$

where $\text{OD}_{570(\text{Sample})}$ represents measurement from the wells containing scaffold and $\text{OD}_{570(\text{Control})}$ from the wells without scaffold. All data are presented as the mean of three measurements (±SD).

2.8.4. Alizarin Red S staining. For Alizarin Red staining, scaffolds were fixed with 3.7% formaldehyde for 1 h at 37 °C and then stained with Alizarin Red S (10 mg mL^{-1}) for 1 h. Scaffolds were washed several times with double distilled water to remove excess stain and air dried. Digital images of stained scaffolds were acquired using a digital camera (DSC-W510, SONY). The chemical composition of the mineral was further confirmed by energy dispersive X-ray (EDX) analysis in SEM.

2.9. *In vivo* biocompatibility

All experiments were approved by the Institutional Animal Ethics Committee of the Indian Institute of Science. Polymer films of BCSM-2_5d were cut into disks (5 mm diameter × 1.5 mm thickness) and sterilized with ethylene oxide gas for 1 day. Two month old Sprague-Dawley rats were anesthetized using Ketamine (75 mg kg^{-1}) and Xylazine (10 mg kg^{-1}) through intraperitoneal route. Disks were implanted subcutaneously by blunt incision in the lower back of the animals using sterile surgical techniques. A sham surgical procedure served as the control. Rats were euthanized at 7, 21, 42 and 77 days. The skin tissue with the implanted disk was harvested and fixed in 10% formalin. The tissue was embedded in paraffin, sectioned and stained with hematoxylin and eosin (H&E) for necroscopy study of the polymer–tissue interface. Liver and kidney were also fixed in 10% formalin, and tissue sections were stained with hematoxylin and eosin (H&E) for histopathological diagnosis.

2.10. Statistics

All the data are reported as the average ± the standard deviation about the average. Statistical differences were determined using a one-way ANOVA and differences were considered significant for p values less than 0.05.
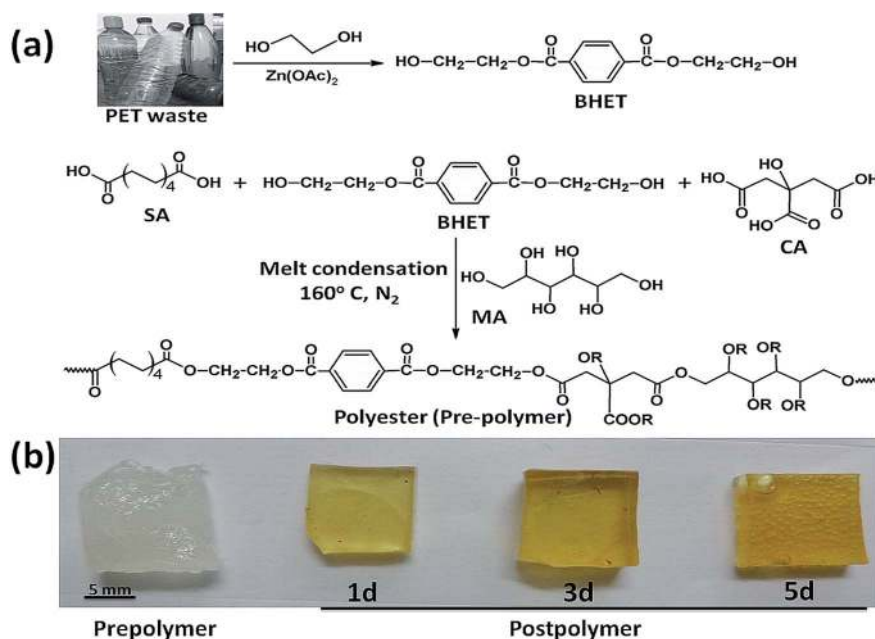

Fig. 1 (a) Synthesis scheme for preparation of BHET monomer and subsequently the pre-polymer, and (b) photographs of the polyester prior to post-polymerization (white, opaque) and after post-polymerization at different post-polymerization times, 1 day (light yellow, transparent), 3 days (brighter yellow, transparent) and 5 days (bright yellow, transparent).

3. Results and discussion

3.1. Synthesis of polyesters

BCSM elastomer was synthesized by a two-stage process (Fig. 1). In the first stage, the pre-polymer was prepared in a one-step catalyst-free, melt-condensation process without the need for severe temperature and pressure reaction conditions. Catalyst-free synthesis is highly desired to minimize potential cytotoxicity arising from the remnant catalyst, which may be toxic for biomedical applications. BCSM polyester was prepared with three different mole ratios of the monomers (Table 1). The pre-polymers were soluble in acetone, dioxane, tetrahydrofuran (THF), dimethyl sulfoxide (DMSO), ethanol and methanol but they were insoluble in water, chloroform and hexane. In the second stage, the pre-polymer was post-polymerized at 120 °C to obtain the final elastomeric polyester. The final post-polymerized polyesters were insoluble in all solvents.

3.2. Structural characterization

Fig. 2a shows the FTIR spectra of PET, BHET and BHET-based all polyesters at 5 days post-polymerization. PET shows a strong peak at 1714 cm^{-1} attributed to C=O stretching of ester group. The C=O peak intensity of ester decreased after glycolysis of PET and a new peak appeared at 3440 cm^{-1} corresponding to the free hydroxyl group in BHET. Along with this, a sharp peak at 723 cm^{-1} is related to the *para* substituted aromatic ring. After post-polymerization, further increase in the peak intensity at 1718 cm^{-1} for C=O stretch of ester group confirms the esterification of BHET with SA and CA. The peaks at 2929 cm^{-1} and 2855 cm^{-1} are assigned to symmetrical and asymmetrical stretching of the CH$_2$ group, respectively. Fig. S1† shows the FTIR spectra of BCSM-2 polyester at different post-polymerization times. A broad peak of O–H stretching at 3411 cm^{-1} in pre-polymer (0 day post-polymerization) indicates the presence of unreacted monomers. The absorption of O–H stretching and C=O stretching of ester gradually decreased and increased, respectively, with increasing post-polymerization time and reached saturation after 5 days.

^{1}H NMR (Fig. 2b) and ^{13}C NMR (Fig. S2†) were used to characterize the purified pre-polymer to confirm the monomer composition in the pre-polymer. Due to overlapping of peaks, the quantification of the monomer ratios in the final polymer from the NMR spectrum was not possible. The peaks were broadened and groups of signals were obtained due to presence of oligomers with different chain lengths in the pre-polymer. The same nuclei can have slightly different chemical shifts due to different neighbouring molecules in the oligomer sequence.[21] The peaks at 8.1, 4.5 and 3.9 ppm are attributed to the presence of BHET monomer in the polymer composition. The unreacted COOH group of SA showed a broad peak at around 9.7 ppm along with the other peaks at 1.3, 1.2 and 2.3 ppm. The methylene protons of citric acid are merged with methylene peaks of SA at 2.7 and 2.6 ppm. In addition, a cluster of peaks for citric acid and mannitol appeared at 2.8–3.1 ppm. The ^{13}C NMR spectrum also confirmed the assumption drawn from the ^{1}H NMR spectrum. Fig. S2† shows a strong peak at 130

ppm that corresponds to the aromatic ring carbons of BHET. The α, β and the remaining methylene carbons of sebacic acid were observed around 24 to 36 ppm.[28] The peaks for carbon atoms of mannitol appeared within 62–65 ppm. The carboxylic carbon peaks for sebacic acid and citric acid were obtained at around 175 ppm and 170 ppm, respectively. A small peak for quaternary carbon was found at around 75 ppm, corresponding to the quaternary carbon in citric acid.[29] It was found that the molecular weight of pre-polymers gradually increased from 386 to 423 to 505 dalton with increase in BHET content.

X-ray diffraction (XRD) pattern of all polyesters at 5 days post-polymerization is shown in Fig. 2c. Fig. 2c shows that the crystallinity peak gradually broadened with increase in the BHET content in the polyester composition due to incorporation of bulky aromatic moiety in the polymer chain which renders the chain alignment. The crystallinity of BCSM-2 polyester gradually decreased with increase in the post-polymerization time (Fig. S3†). All polyesters were prepared by crosslinking the pre-polymers at 120 °C. The pre-polymer of BCSM-2 polyester was post-polymerized for different durations (1 day to 5 days) to study the effect on polymer properties. The other two compositions were post-polymerized for 5 days. After post-polymerization, all crosslinked polyester elastomers were transparent (Fig. 1b).

3.3. Mechanical properties

Tensile stress–strain curves and the values of Young's modulus, ultimate tensile strength and tensile strain of different polyesters at 5 days post-polymerization are shown in Fig. 3a and Table 1, respectively. Fig. 3a shows that both Young's modulus and tensile strength of the polyesters gradually decreased from 3.03 and 3.27 to 0.15 and 0.49 MPa, respectively, with increase in BHET content. However, the ductility increased from 139% to 607%. This is because the crystallinity of the polyester decreased with increased BHET content due to incorporation of bulky aromatic rings in the polymer. On the other hand, it was found that the ultimate tensile strength (UTS) and Young's modulus of BCSM-2 polyester increased from 0.42 to 2.31 MPa and 0.16 to 1.84 MPa, respectively, with increase in the duration of post-polymerization (crosslinking). The percent elongation at break decreased from 388 ± 27% to 167 ± 11% (Fig. S4†). This is due to increase in the crosslinking density with increasing post-polymerization time.

Poly(glycerol sebacate) polyester elastomer[30] showed moderate mechanical properties having Young's modulus, tensile stress and tensile strain of ~0.282 MPa, ~0.5 MPa, and ~267%, respectively. In another study, poly(xylitol sebacate) polyesters[31] was prepared by varying the molar content of diacid. The polyester exhibited Young's modulus, ultimate tensile strength (UTS) and elongation at break of 0.82–5.33 MPa, 0.61–1.43 MPa and 33–205%, respectively. Polyester elastomer containing hydrolytically stable amide bonds were synthesized to enhance *in vivo* degradation rate.[32] These polyesters had Young's moduli, UTS, and tensile strain ranging from 1.45–4.34 MPa, 0.24–1.69 MPa and 21–92%, respectively. Citric acid based biodegradable elastomers[33] showed Young's modulus and
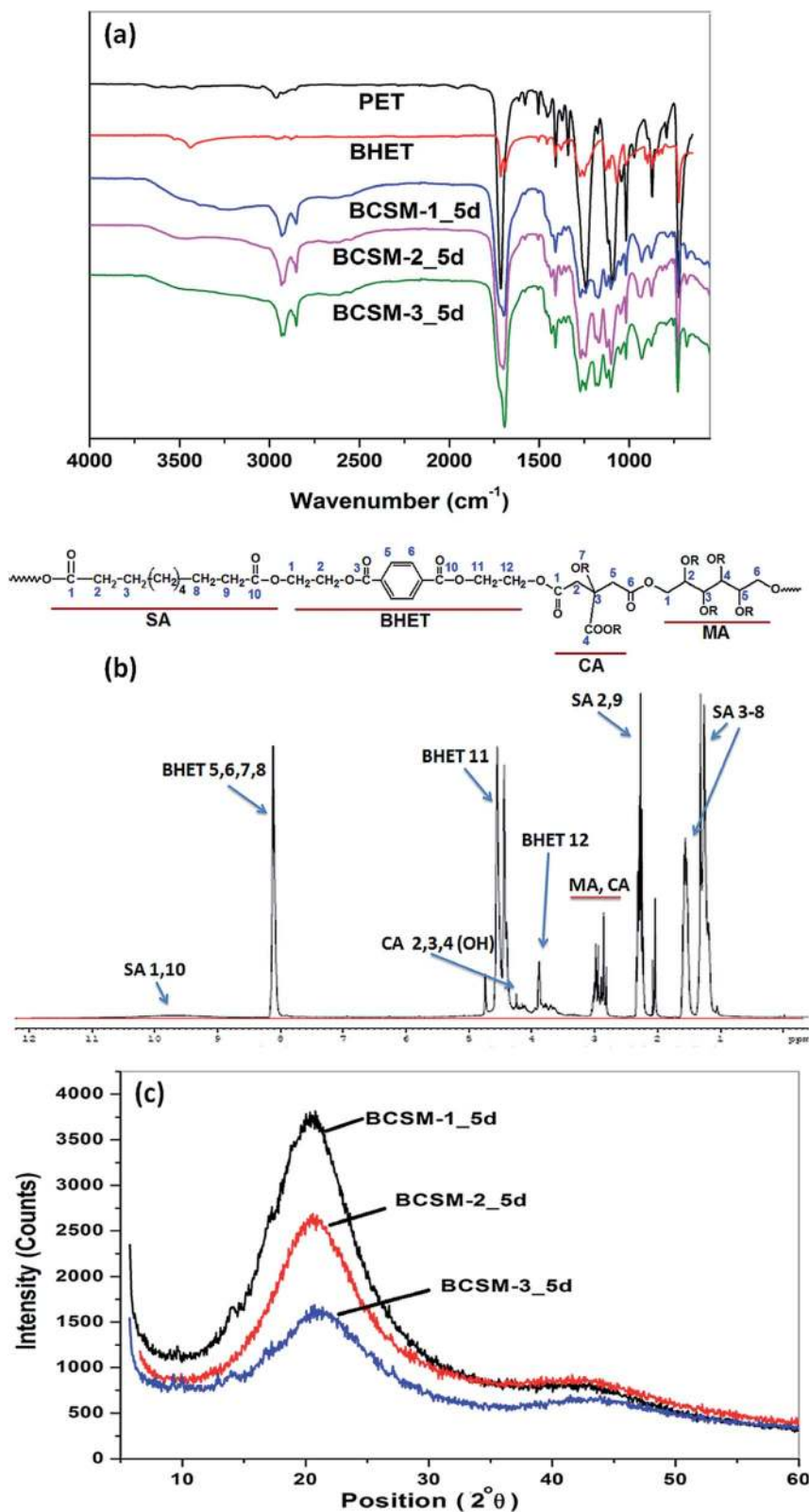
Fig. 2 Chemical characterization of different polyester elastomers at 5 days post-polymerization. FTIR spectra of PET, BHET and all polyesters at 5 days post-polymerization (a); ^{1}H NMR spectra of purified BCSM-2 pre-polymer (b) and X-ray diffraction patterns of all polyesters at 5 days post-polymerization (c).

tensile strain of the elastomer increased and decreased, respectively with increase in the post-polymerization time. In this work, we have synthesized novel polyesters by solvent and catalyst free method using recycled consumer PET waste, which is not only economical but also eco-friendly. This polyester has equivalent or better mechanical properties compared to the previously synthesized polyesters. There are many soft tissues such as articular cartilage (Young's modulus – 2.1–11.8 MPa; tensile strength – 9–40 MPa, tensile strain – 60–120%), aorta (Young's modulus – 2.0–6.5 MPa; tensile strength – 0.3–0.8 MPa, tensile strain – 50–100%), smooth muscle (Young's modulus – 0.01–0.006 MPa; tensile strain – 300%) where the mechanical properties are quite similar to that of synthesized BHET based

polyester in this work. Thus, this class of BHET-based polymers could be developed for use in repair and regeneration of different tissues. The mechanical properties can be appropriately tuned by varying the composition and curing conditions.

3.4. Thermal properties

The differential scanning calorimetry (DSC) measurements of all polyesters at 5 days post-polymerization is shown in Fig. 3b. The DSC thermogram does not show any crystallization and melting temperature demonstrating that the polymers are not crystalline in nature. All polyesters show that the glass transition temperatures (T_g) were below room temperatures (−10 °C to +10 °C) indicating that all polyesters are elastomeric at 37 °C.
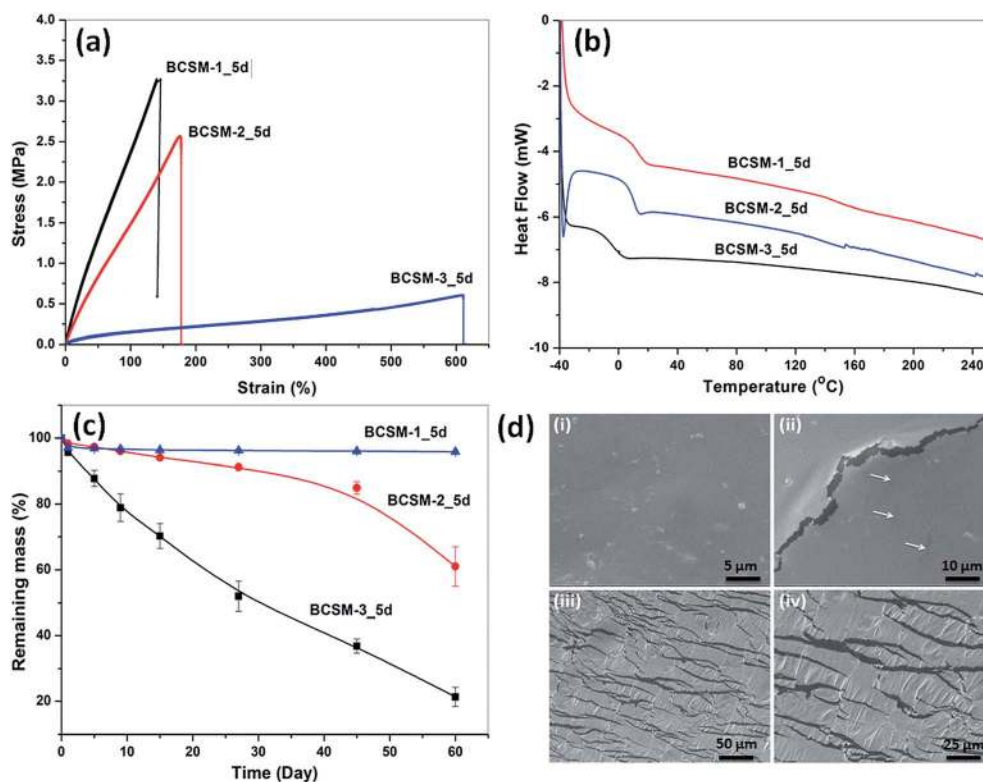

Fig. 3 Representative stress–strain plots of different polyesters with varying BHET contents after 5 days post-polymerization (a); DSC thermograms of different polyesters with varying BHET contents after 5 days post-polymerization (b); in vitro hydrolytic degradation profile of different polyesters with varying BHET contents after 5 days post-polymerization (c) and SEM images of degraded polyester film surfaces of BCSM-2 after 5 days post-polymerization (d) after 1 day (i), 7 day (ii) and 14 day; 300× mag. (iii) and 600× mag. (iv).
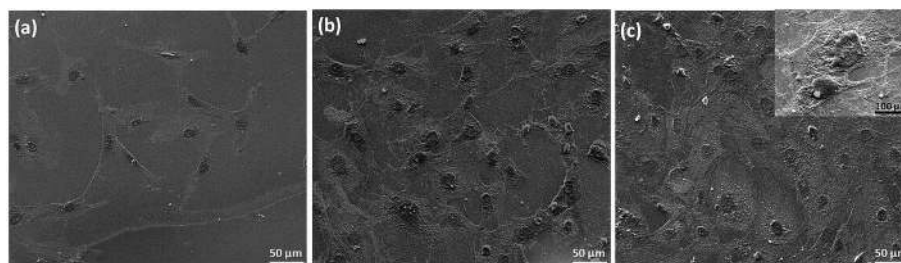

Fig. 4 Cell attachment and proliferation on BCSM-2 polyester films after 5 days post-polymerization. SEM micrographs of MC3T3-E1 osteoblast cells on polyester film at (a) 1 day, (b) 3 days and (c) 7 days. The dimension of the film sample was 5 × 5 mm² and 1 mm thickness.
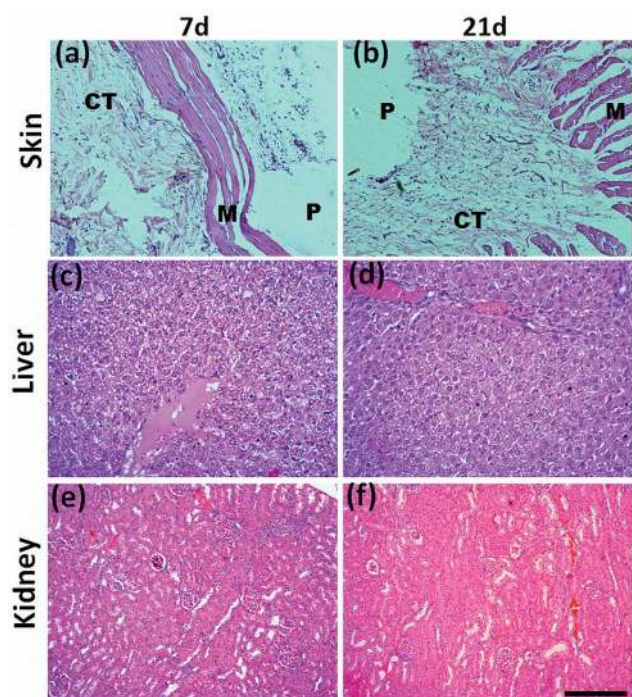
Fig. 5 Photographs of Sprague-Dawley rat subcutaneous tissue response at 7 days (a) and 21 days (b) after implantation, showing loose connective tissue matrix surrounding the implant with moderate inflammation and infiltration of inflammatory cells. Histopathological micrographs of liver and kidney at 7 days (c and e) and 21 days (d and f), respectively. The dimension of implanted sample was 5 mm diameter and 2 mm thickness. M = muscular tissue, CT = connective tissue, P = polyester. Scale bar is 50 μm.

BCSM-3 polyester showed the lowest glass transition temperature among the all polyesters due to its more amorphous nature caused by higher BHET content. The glass transition value gradually decreased with increase in BHET content due to the presence of bulky aromatic ring in BHET monomer that hinders the polymer chain alignment to form a crystalline structure.

3.5. Surface wettability

The biological response to a material is known to depend on the hydrophobicity of its surface. From Table 1, it was found that the water-in-air contact angle gradually increased as expected from 60.5 to 85.4° with increase in the BHET content in the polyester due to increase in the hydrophobic aromatic content presented in BHET. The effect of curing time on water-in-air contact angle of polymer was also observed. The contact angle of BCSM-2 at 3 days post-polymerization was comparatively low at 68.7° due to the presence of unreacted hydroxyl groups. But the contact angle gradually increased from to 72.8° and 76.9° after 4 days and 5 days post-polymerization, respectively, due to the decrease in the availability of free hydroxyl groups because of the condensation reaction with carboxyl groups. The degradation rate of biomaterials is also influenced by its water wettability.

3.6. *In vitro* degradation

Hydrolytic degradation of the polyester elastomer in PBS at 37 °C was studied *in vitro*. The degradation profile of all polyesters at 5 days post-polymerization is presented in Fig. 3c. It was found that the degradation rate of polyester can be modulated by varying the BHET content. Increased BHET content decreased degradation rates due to the hydrophobicity of the aromatic ring in BHET. The effect of post-polymerization time on *in vitro* degradation rate of the polymer was also studied. Fig. S5† illustrates the *in vitro* degradation profile of BCSM-2 polyester with varying post-polymerization time. It was observed that BCSM-2 post-polymerized for 1 day degraded completely in 18 days whereas the polyester post-polymerized for 4 days and 5 days showed only 15% and 9% degradation, respectively, in 30 days. Therefore, the degradation rate of the polyester can be tuned by varying the duration of post-polymerization because the crosslinking density of elastomer scales with the curing time. SEM images (Fig. 3d) revealed fine cracks on the surface of the elastomer at 1 day (Fig. 3d(ii)) which progressively developed into deeper cracks by 10 days (Fig. 3d(iii)) indicating bulk degradation in contrast to surface erosion as the underlying mechanism.

3.7. *In vitro* and *in vivo* biocompatibility of polyesters

BCSM-2_5d polyester was used in all *in vitro* and *in vivo* studies because of its optimal mechanical properties (Young's modulus – 1.84 MPa, tensile strength – 2.31 MPa and tensile strain – 168%), moderate surface wettability (contact angle – 77°) and
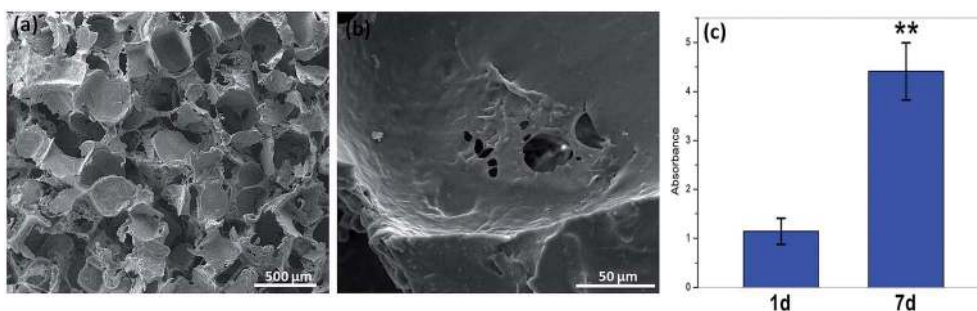

Fig. 6 SEM micrographs of as-prepared 3D porous scaffold (a), cell attachment with 3D scaffold (b) and cell proliferation on 3D scaffold at 1 day and 7 days (c). The dimension of 3D scaffold was 6 mm diameter and 3 mm thickness.

Paper

RSC Advances

medium degradation rate (60% degradation after 60 days). To evaluate the cytocompatibility of the polyester elastomer *in vitro* and specifically its potential in orthopaedics, mouse osteoblasts were cultured on BCSM-2_5d polymer films. SEM micrographs show that cells were attached and spread on the polymer film at

1 day (Fig. 4a). Cells were observed to be connected to each other through the long axis of the cell body. Increased number of cells seen at 3 days and 7 days (Fig. 4b and c, respectively) indicated that the polymer supported cell proliferation and is thus cytocompatible. Cell morphology is important in
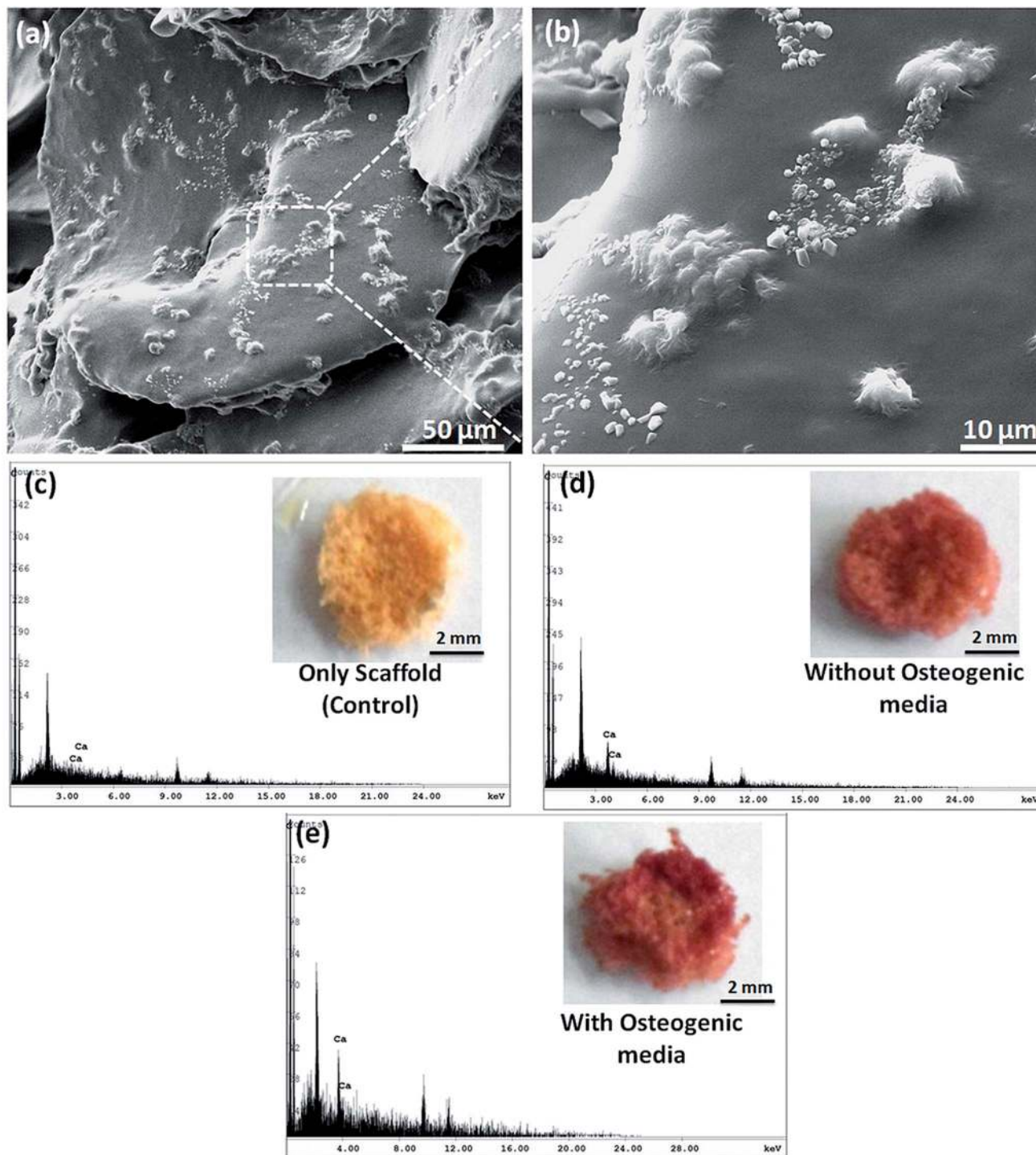
Fig. 7   SEM micrographs of 3D scaffold showing mineral deposition after 7 days of cell culture at 500× (a) and 2000× magnification (b). EDAX spectra of mineralized scaffold, before cell culture (c), cell culture without osteogenic supplement in media (d) and with osteogenic supplement in media (e) at 7 days with inset displaying the photograph of the scaffold stained with Alizarin Red S dye. The dimension of 3D scaffold was 6 mm diameter and 3 mm thickness.

determining its fate and function, including survival, migration, proliferation, and differentiation.[34,35] Most cells on the polyester film spread radially in all directions and several filopodia of the spread cells were also observed (inset, Fig. 4c).

Biocompatibility of the polyester elastomer was further assessed by subcutaneous implantation of BCSM-2_5d in a rat model. Acute and chronic inflammation up to 77 days was assessed by histology of the polymer–tissue interface, liver and kidney, (Fig. 5) and was compared to those in sham surgery (Fig. S6†). Representative images of the skin in the vicinity of implant after 7 days and 21 days (Fig. 5a and b, respectively) showed normal architecture of epidermis and dermis similar to that in the sham (Fig. S6a and S6b,† respectively). Histopathological investigation of the liver (Fig. 5c and d) and kidney (Fig. 5e and f) did not suggest any toxicity associated with the implanted polymer. The dermis also appeared normal without any leukocyte infiltration denoting absence of inflammation and the skin adnexa were also normal at 42 days and 70 days (not shown).

Three-dimensional (3D) macroporous scaffolds were prepared by the widely-used salt leaching method wherein NaCl was used the porogen.[36] SEM micrographs in Fig. 6a show the interconnected porous architecture of the 3D scaffold. The porosity of the all scaffolds was $85 \pm 6\%$, and the average pore size was 400 ± 25 μm (Table 1) which is the recommended size range for bone tissue engineering.[37] Micropores within the macropores were also observed and may enhance the transportation of nutrient within the scaffold. Osteoblasts in the BCSM-2_5d scaffolds were full stretched morphology (Fig. 6b) such that it was difficult to discern the boundary between the cell membrane and polymer. Cell attachment and proliferation in the scaffolds were quantified by MTT assay at 1 day and 7 days, respectively (Fig. 6c). The four-fold increase in absorbance from 1 day to 7 days indicates that these scaffolds supported proliferation of the osteoblasts. Interestingly, SEM images (Fig. 7a and b) showed mineral deposition in the scaffold at 7 days even in the absence of osteogenic supplement. Alizarin S staining also confirmed the formation of mineral deposits in the scaffolds at 7 days (inset, Fig. 7d and e). The distinct calcium peak at 3.7–3.8 keV in the EDAX spectra corroborated the formation of calcium phosphate deposition (Fig. 7d and e), although the peak intensity was higher in presence of osteogenic media indicating more deposition of calcium phosphate. Thus, BCSM scaffolds are well suited for bone regeneration applications.

Previously, Langer and co-workers have prepared poly(glycerol sebacate) (PGS) polyester by random polycondensation reactions between glycerol and sebacic acid for several followed by post-polymerization.[4] Ameer and co-workers have reported on the preparation of poly(1,8-octane citrate) (POC) polyester for preparing small diameter blood vessels.[38] In this work, we have prepared the BCSM polyester elastomer by random polycondensation reaction. In contrast to the other polymers, we have utilized BHET derived from recycled consumer PET waste demonstrating the use of recycled plastic waste for developing affordable healthcare solutions. Thus, BHET-based polyesters could serve as low cost, eco-friendly, biocompatible and biodegradable polymers for possible biomedical applications.

4. Conclusions

We have synthesized a novel polyester elastomer using BHET monomer from recycled PET waste and other monomers derived from low cost, renewable sources including SA, CA and MA. The synthesis of this polyester elastomer is simple, eco-friendly and cost effective. A wide range of mechanical properties and degradation rates were obtained just by tuning the monomer feed ratios and the post-polymerization times. The elastomer showed excellent cytocompatibility *in vitro* and elicited little immune response *in vivo*. 3D porous scaffolds facilitated osteogenic differentiation and mineralization. Therefore, the polyester can be used as soft tissue engineering application and it may be also used in bone tissue engineering application after further improvement of its mechanical properties.

Acknowledgements

References

1 J. Bonadio, E. Smiley, P. Patil and S. Goldstein, *Nat. Med.*, 1999, **5**, 753–759.

2 D. W. Hutmacher, *J. Biomater. Sci., Polym. Ed.*, 2001, **12**, 107–124.

3 S. Yang, K.-F. Leong, Z. Du and C.-K. Chua, *Tissue Eng.*, 2002, **8**, 1–11.

4 Y. Wang, G. A. Ameer, B. J. Sheppard and R. Langer, *Nat. Biotechnol.*, 2002, **20**, 602–606.

5 S. Chaudhary, P. Surekha, D. Kumar, C. Rajagopal and P. K. Roy, *J. Appl. Polym. Sci.*, 2013, **129**, 2779–2788.

6 I. Vitkauskiene and R. Makuska, *Chemija*, 2008, **19**, 29–34.

7 G. P. Karayannidis, A. K. Nikolaidis, I. D. Sideridou, D. N. Bikiaris and D. S. Achilias, *Macromol. Mater. Eng.*, 2006, **291**, 1338–1347.

8 C. N. Hoang and Y. H. Dang, *Polym. Degrad. Stab.*, 2013, **98**, 697–708.

9 L. Zhang, J. Gao, J. Zou and F. Yi, *J. Appl. Polym. Sci.*, 2013, **130**, 2790–2795.

10 D. Carta, G. Cao and C. D'Angeli, *Environ. Sci. Pollut. Res.*, 2003, **10**, 390–394.

11 I. Acar and M. Orbay, *Polym. Eng. Sci.*, 2011, **51**, 746–754.

12 M. S. Farahat, *Polym. Int.*, 2002, **51**, 183–189.

13 P. Czub, *Polym. Adv. Technol.*, 2009, **20**, 183–193.

14 M. S. Farahat and D. E. Nikles, *Macromol. Mater. Eng.*, 2001, **286**, 695–704.

15 J. Hiremath, V. Kusum Devi, K. Devi and A. Domb, *J. Appl. Polym. Sci.*, 2008, **107**, 2745–2754.

16 N. Kumar, R. S. Langer and A. J. Domb, *Adv. Drug Delivery Rev.*, 2002, **54**, 889–910.

17 S. Pasupuleti, A. Avadanam and G. Madras, *Polym. Eng. Sci.*, 2011, **51**, 2035–2043.

18 P. Sathiskumar and G. Madras, *Polym. Degrad. Stab.*, 2011, **96**, 1695–1704.

19 D. G. Barrett and M. N. Yousaf, *Molecules*, 2009, **14**, 4022–4050.

20 P. T. Riquelme, M. E. Wernette-Hammond, N. M. Kneer and H. A. Lardy, *Proc. Natl. Acad. Sci.*, 1983, **80**, 4301–4305.

21 F. Barroso Bujans, R. Martinez and P. Ortiz, *J. Appl. Polym. Sci.*, 2003, **88**, 302–306.

22 M. Ghaemy and F. Behzadi, *Iran. Polym. J.*, 2002, **11**, 77–83.

23 U. Vaidya and V. Nadkarni, *J. Appl. Polym. Sci.*, 1988, **35**, 775–785.

24 S. Pasupuleti and G. Madras, *J. Appl. Polym. Sci.*, 2011, **121**, 2861–2869.

25 G. Kumar, C. K. Tison, K. Chatterjee, P. S. Pine, J. H. McDaniel, M. L. Salit, M. F. Young and C. G. Simon Jr, *Biomaterials*, 2011, **32**, 9188–9196.

26 R. Zhang and P. X. Ma, *J. Biomed. Mater. Res.*, 1999, **44**, 446–455.

27 L. D. Quarles, D. A. Yohay, L. W. Lever, R. Caton and R. J. Wenstrup, *J. Bone Miner. Res.*, 1992, **7**, 683–692.

28 E. Ron, E. Mathiowitz, G. Mathiowitz, A. Domb and R. Langer, *Macromolecules*, 1991, **24**, 2278–2282.

29 D. Gyawali, P. Nair, Y. Zhang, R. T. Tran, C. Zhang, M. Samchukov, M. Makarov, H. K. Kim and J. Yang, *Biomaterials*, 2010, **31**, 9092–9105.

30 Y. Wang, G. A. Ameer, B. J. Sheppard and R. Langer, *Nat. Biotechnol.*, 2002, **20**, 602.

31 J. P. Bruggeman, C. J. Bettinger, C. L. E. Nijst, D. S. Kohane and R. Langer, *Adv. Mater.*, 2008, **20**, 1922.

32 C. J. Bettinger, J. P. Bruggeman, J. T. Borenstein and R. Langer, *Biomaterials*, 2008, **29**, 2315.

33 J. Yang, A. R. Webb and G. A. Ameer, *Adv. Mater.*, 2004, **16**, 511.

34 F. Guilak, D. M. Cohen, B. T. Estes, J. M. Gimble, W. Liedtke and C. S. Chen, *Cell Stem Cell*, 2009, **5**, 17–26.

35 A. S. Andersson, F. Backhed, A. von Euler, A. Richter Dahlfors, D. Sutherland and B. Kasemo, *Biomaterials*, 2003, **24**, 3427–3436.

36 K. Chatterjee, S. Hung, G. Kumar and C. G. Simon, *J. Funct. Biomater.*, 2012, **3**, 372–381.

37 L. Cyster, D. Grant, S. Howdle, F. Rose, D. Irvine, D. Freeman, C. Scotchford and K. Shakesheff, *Biomaterials*, 2005, **26**, 697–702.

38 J. Yang, A. R. Webb and G. A. Ameer, *Adv. Mater.*, 2004, **16**, 511–516.